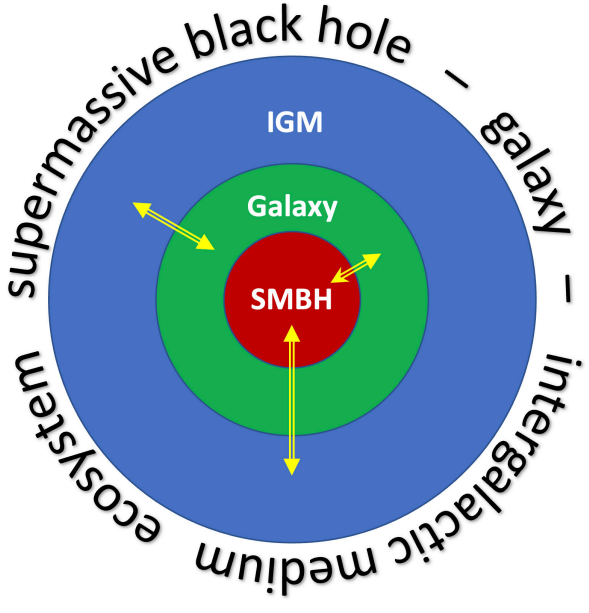
External Negative Feedback on Galaxy Formation from Giant Radio Lobes



Renyue Cen (岑人岳)

Center for Cosmology and Computational Astrophysics (C^3A)

Institute for Advanced Study in Physics

&

Institute of Astronomy

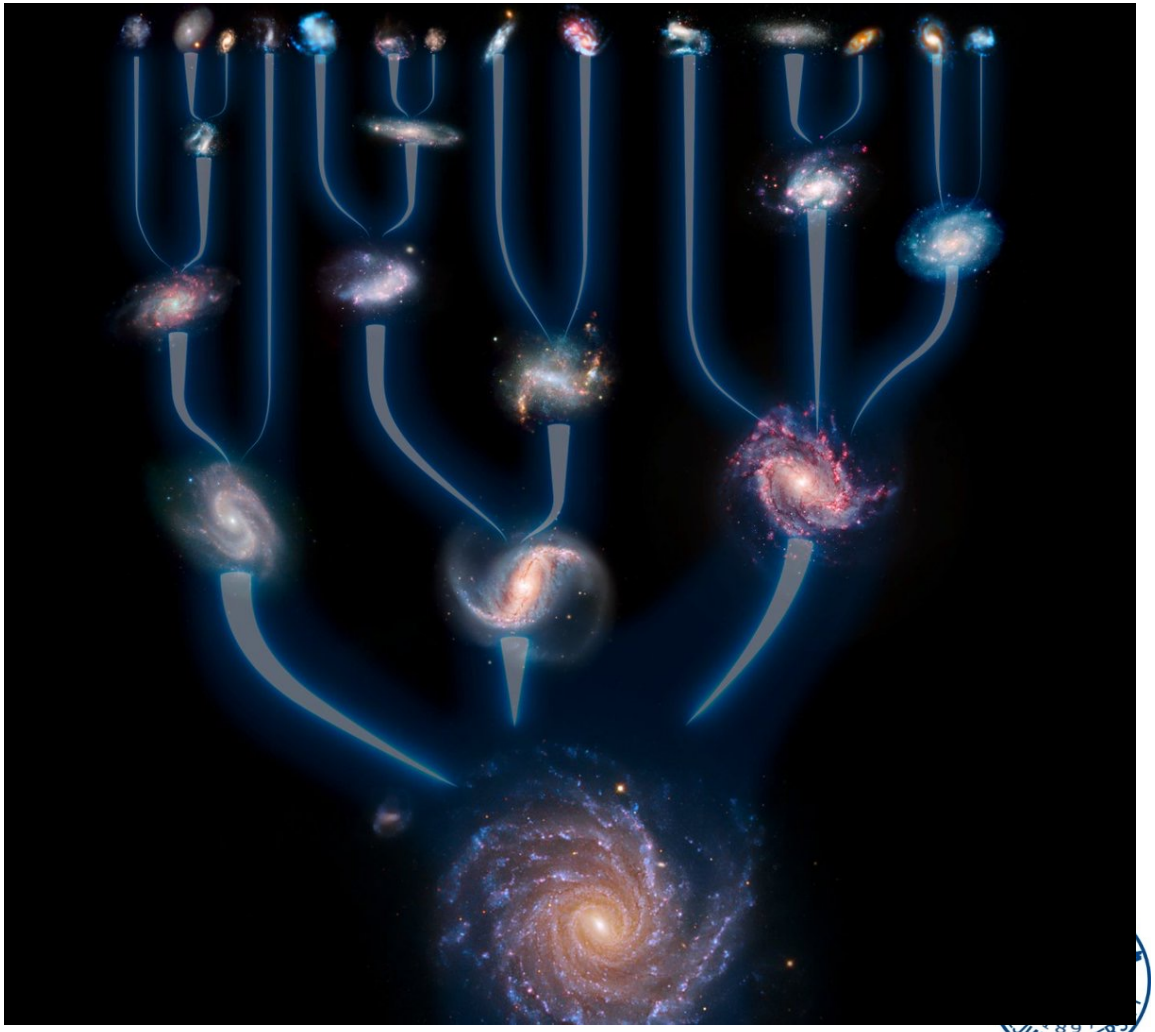
School of Physics

Zhejiang University

@11th KIAS Workshop, 2024年11月1日

The virialization of dark matter particles

- Most of the dark matter has been in halos since 1st generation of halos formed @z=20-30.



Galaxy formation : if unhindered

Earlier simulations (e.g., Cen 1990, 100^3 simulation) show, without additional negative feedback:

$\Omega_* \approx \Omega_b/3$ vs observed $\Omega_* = 8\% \, \Omega_b$

The merging history of dark matter halos

- Milky Way size dark matter halos have had 20 doublings of their masses down to z=0 since z=20-30.

- Most dark matter halos have had experienced on order of 10 significant mergers since.

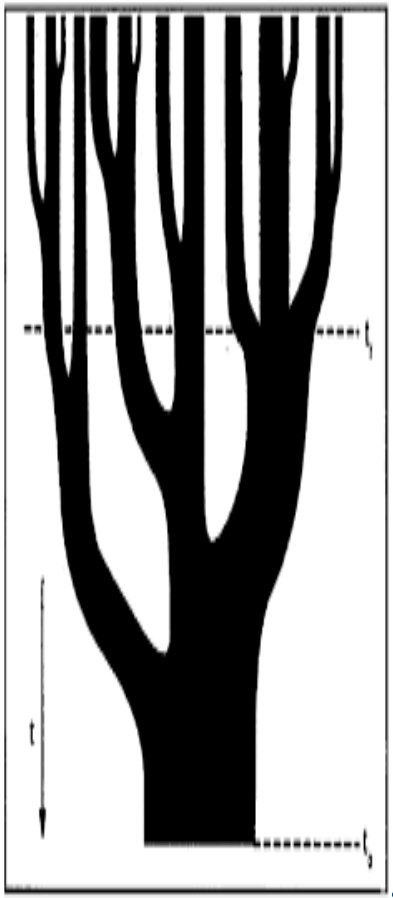
Baryons in halos： baryons had time to form stars, if unhindered

- ***if all baryons had followed their fellow dark matter particles***,

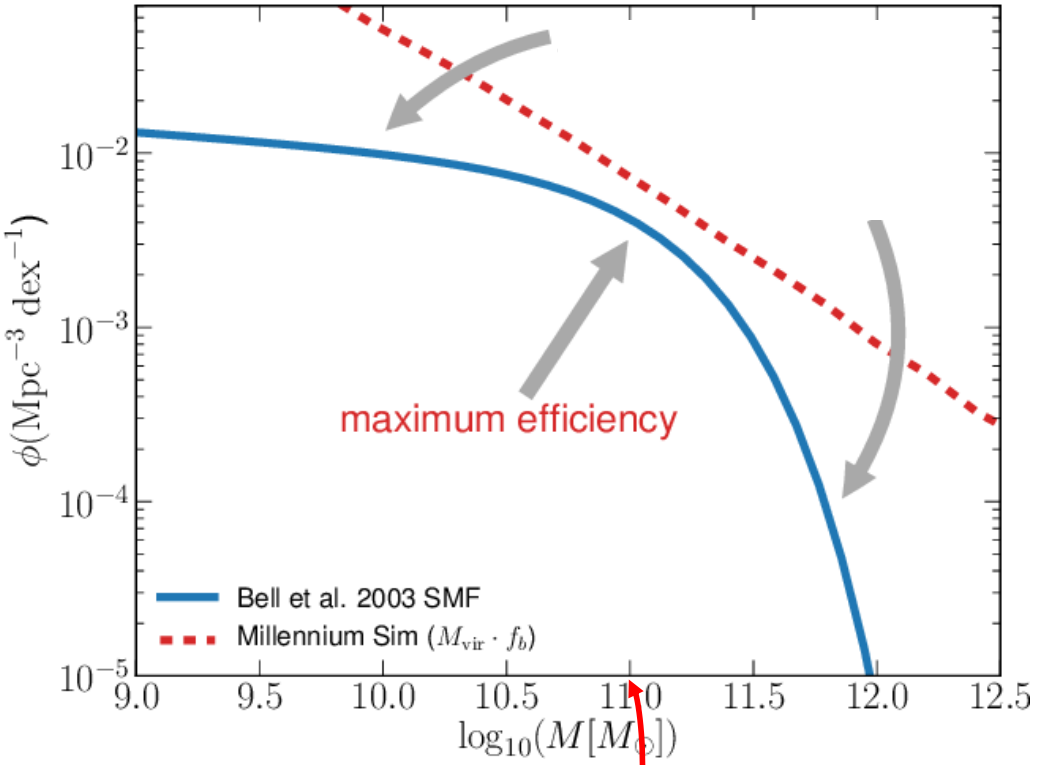
a baryon apparently on average had

<1% chance to have been turned into stars

on each merging branch when climbing down the tree



How many kinds of negative feedback needed?



Clearly, *at least two different* kinds of feedback processes must be operating, because

- **The effect is non-monotonic as a function of the halo mass:**

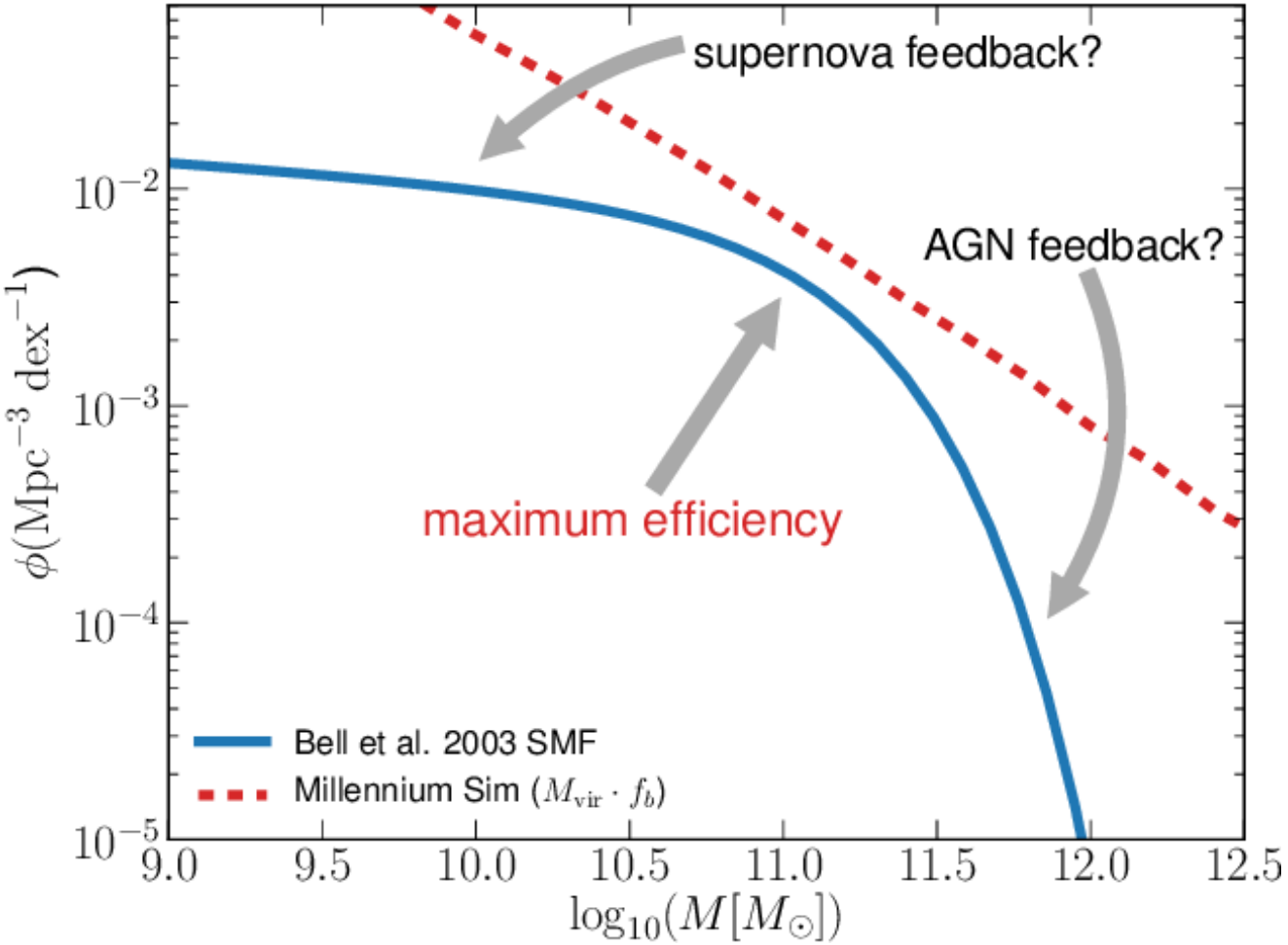
increases towards the high mass end

increases towards the low mass end

- **There is an apparent minimum of suppression effect at around**

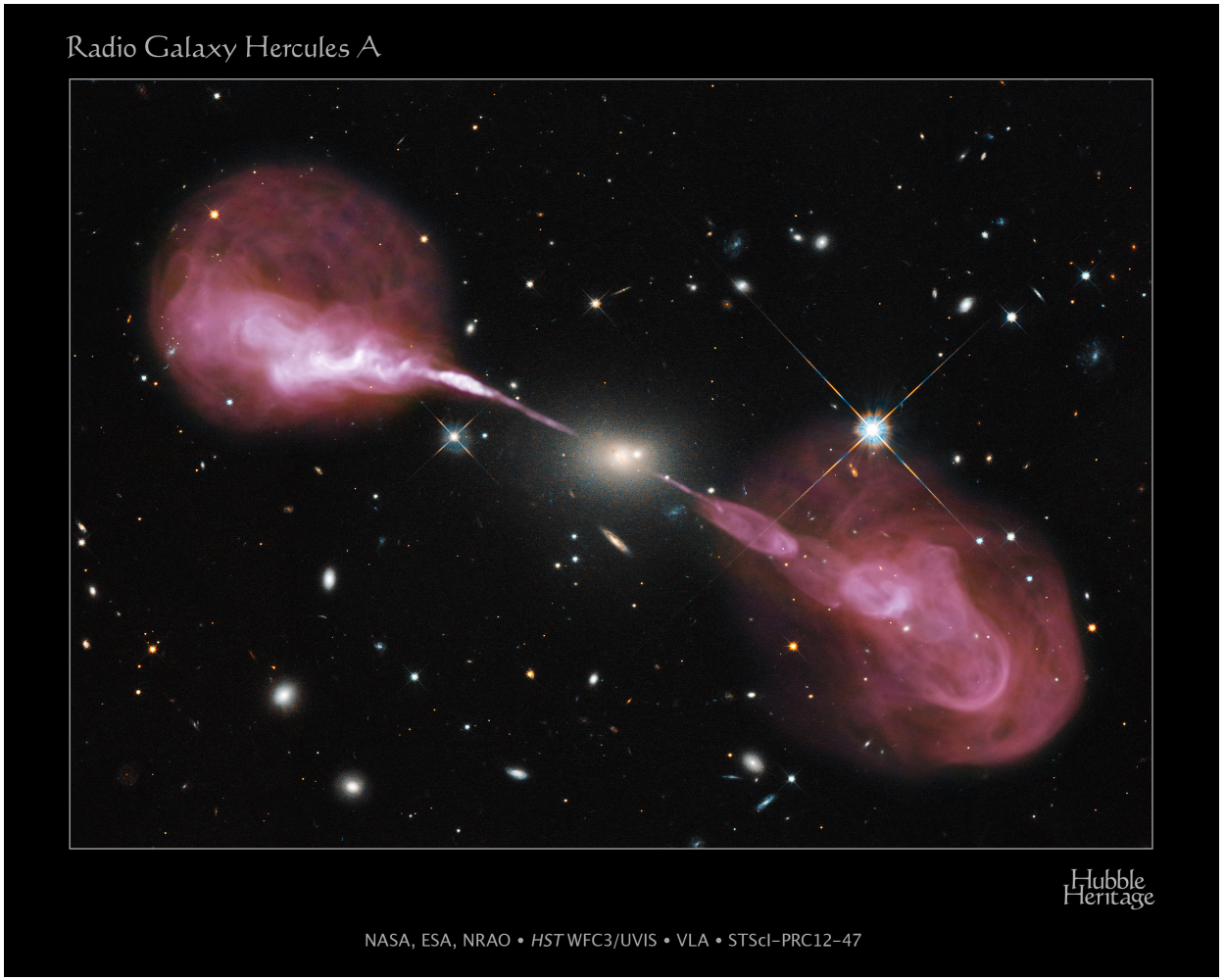
M_h=10^{12}-$10^{12.5}$M

Main ideas : negative supernova and AGN feedback



On surface, they appear plausible.

How about radio jets: deposit most of energy as far as 1 Mpc



Mechanical energy output:

Table 1
Comparison of SF and SMBH Energetics

No.	Form	SF	SMBH
(1)	Total radiation	$\epsilon_*(\mathrm{rad}) = 7 \times 10^{-3}$	$\epsilon_{\mathrm{BH}}(\mathrm{rad}) = 2 \times 10^{-4}$
(2)	Ionizing radiation ($\geqslant$13.6 eV)	$\epsilon_*(\mathrm{LL}) = 1.4 \times 10^{-4}$	$\epsilon_{\mathrm{BH}}(\mathrm{LL}) = 3 \times 10^{-5}$
(3)	X-ray (2–10 keV)	ϵ_*(2–10 keV) $= 9 \times 10^{-8}$	$\epsilon_{\mathrm{BH}}(2\text{–}10\,\mathrm{keV}) = 5 \times 10^{-6}$
(4)	Mechanical	$\epsilon_*(\mathrm{SN}) = 1 \times 10^{-5}$	ϵ_{BH}(BAL) $= (0.2\text{–}2.8) \times 10^{-5}$
(5)	Radio jets	$\epsilon_*(\mathrm{jet}) = 0$	$\epsilon_{\mathrm{BH}}(\mathrm{jet}) = 4 \times 10^{-5}$

Notes. Under the assumption that M_{BH}: M_{BG} = 2:1000, a Salpeter IMF for stars and a radiative efficiency of SMBH accretion of 10% (Yu & Tremaine 2002), and energy output from both SF and SMBH in various forms are listed: (1) total radiation energy, (2) ionizing radiation, (3) X-ray radiation in the 2–10 keV band, (4) mechanical energy, and (5) radio jets.

$$E_{SN} = 10^{-5}\, M_*\, c^2 \quad \text{v.} \quad E_{AGNjet} = 4\times10^{-5}\, M^*\, (500 M_{BH}/M_*)(e_{jet}/0.2\%)c^2$$

Cen 2012

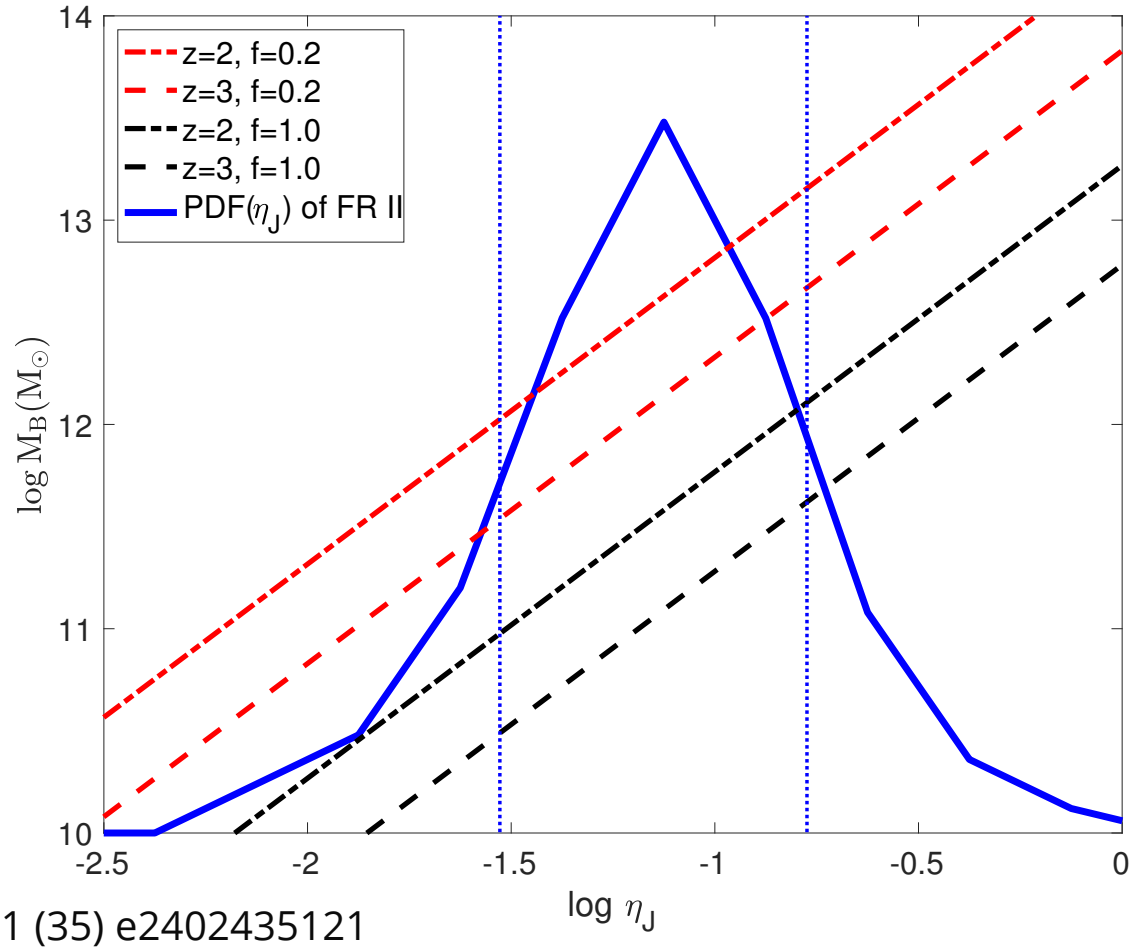
Magnetic field in IGM due to giant radio jets

$$\frac{B_i^2}{8\pi} = 3\times10^{-4}\left(\frac{\eta_{\rm M}}{0.002}\right)\left(\frac{\eta_B}{0.15}\right)\left(\frac{\eta_R}{0.2}\right)\left(\frac{f}{0.2}\right)^{-1}\eta_*\eta_J c^2\rho_b(z)$$
$$= 2.8\times10^{-15}(\mu{\rm G})^2\left(\frac{\eta_{\rm M}}{0.002}\right)\left(\frac{\eta_B}{0.15}\right)\left(\frac{\eta_R}{0.2}\right)\left(\frac{f}{0.2}\right)^{-1}$$
$$\times\left(\frac{\eta_*}{0.018}\right)\left(\frac{\eta_J}{0.05}\right)\left(\frac{1+z}{3}\right)^3, \qquad [3]$$

η_M= SMBH to bulge stellar mass ratio
η_B = fraction of magnetic energy retained through lobe evolution
η_R = radio loud fraction
f = radio lobe volume filling factor
η_* = fraction of baryons formed into stars
η_J = fraction of SMBH rest mass in form of radio lobe in radio loud galaxies

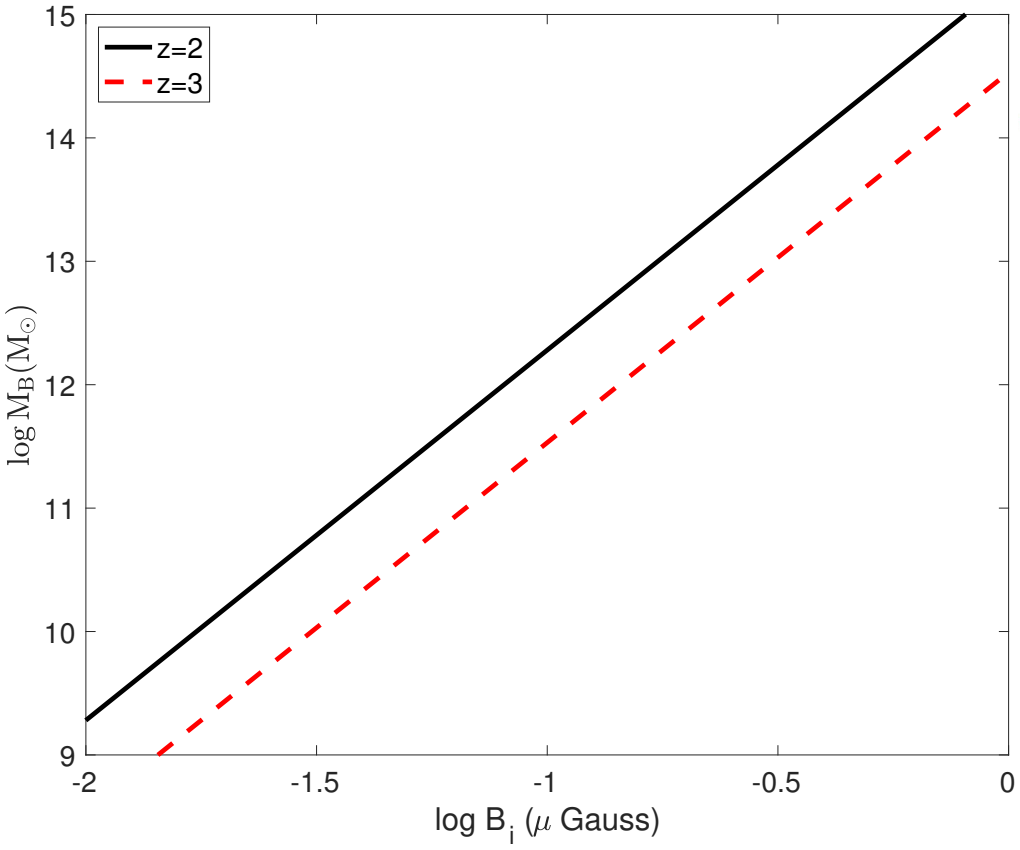
Cen 2024, PNAS, 121 (35) e2402435121

Observed fractional radio energy and expected Jeans mass M_B



Cen 2024, PNAS, 121 (35) e2402435121

Magnetic Jeans scale



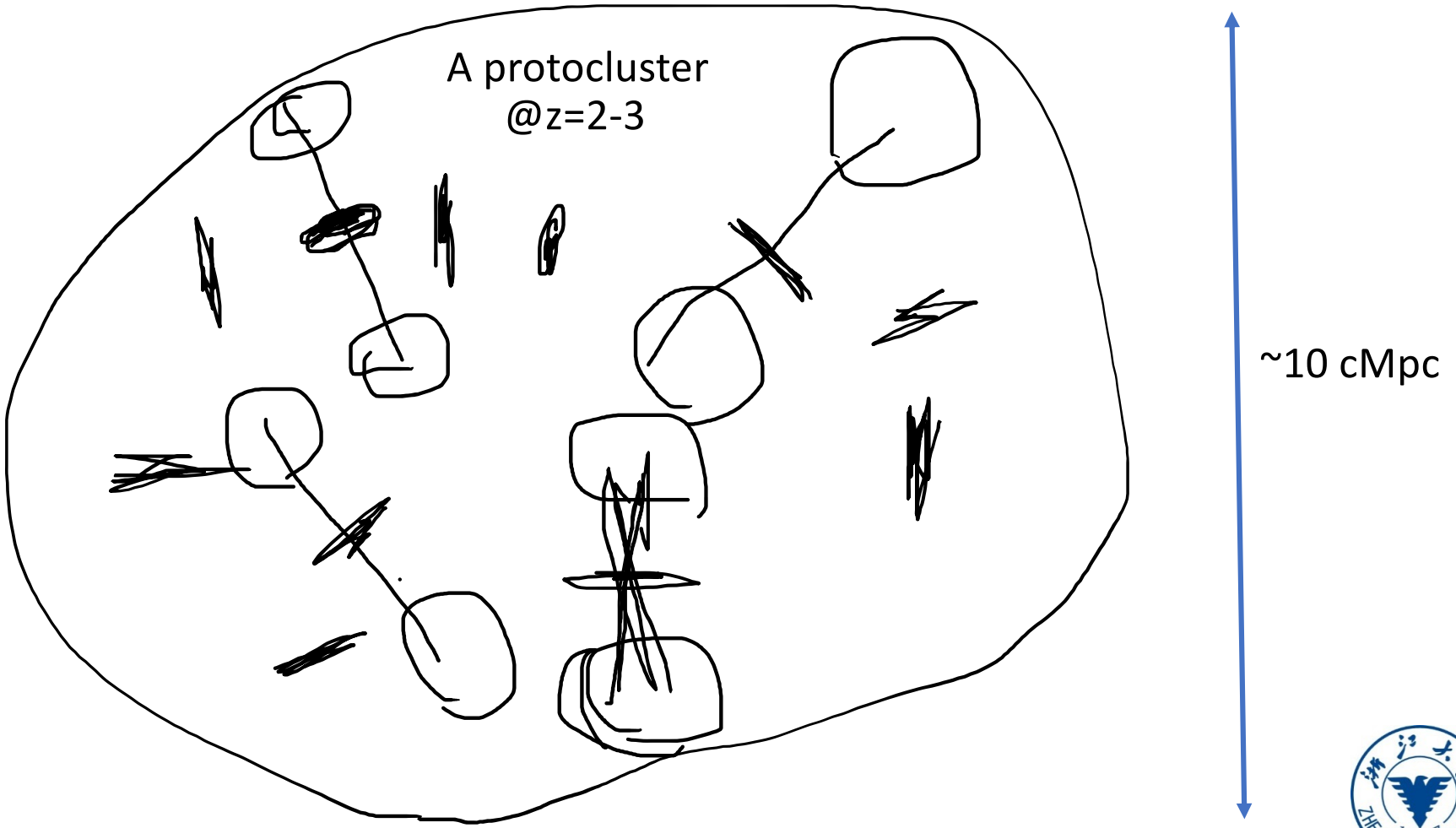
Alfvén velocity $v_A = \sqrt{B_v^2/4\pi\rho_v}$

$= \sqrt{2}\sigma_v$

σ_v is the 1-d velocity dispersion

Cen 2024, PNAS, 121 (35) e2402435121

Radio lobe feedback: external, global, multi-generational



When did magnetic Jeans smoothing kick in?

- It kicks in at z<2,
when most of the AGN jets have formed

- This may solve long standing puzzle of galaxy luminosity function evolution.

Cen 2024, PNAS, 121 (35) e2402435121

Observed evolution of galaxy luminosity function

Galaxy luminosity functions $n(L)\,dL = L^{\alpha}\,dL$

$\alpha \approx -2$ @z > 3

$\alpha \approx -1$ @z = 0

Observations indicate there is a relatively quick change of α from -3 to -1, occurring around z=2:

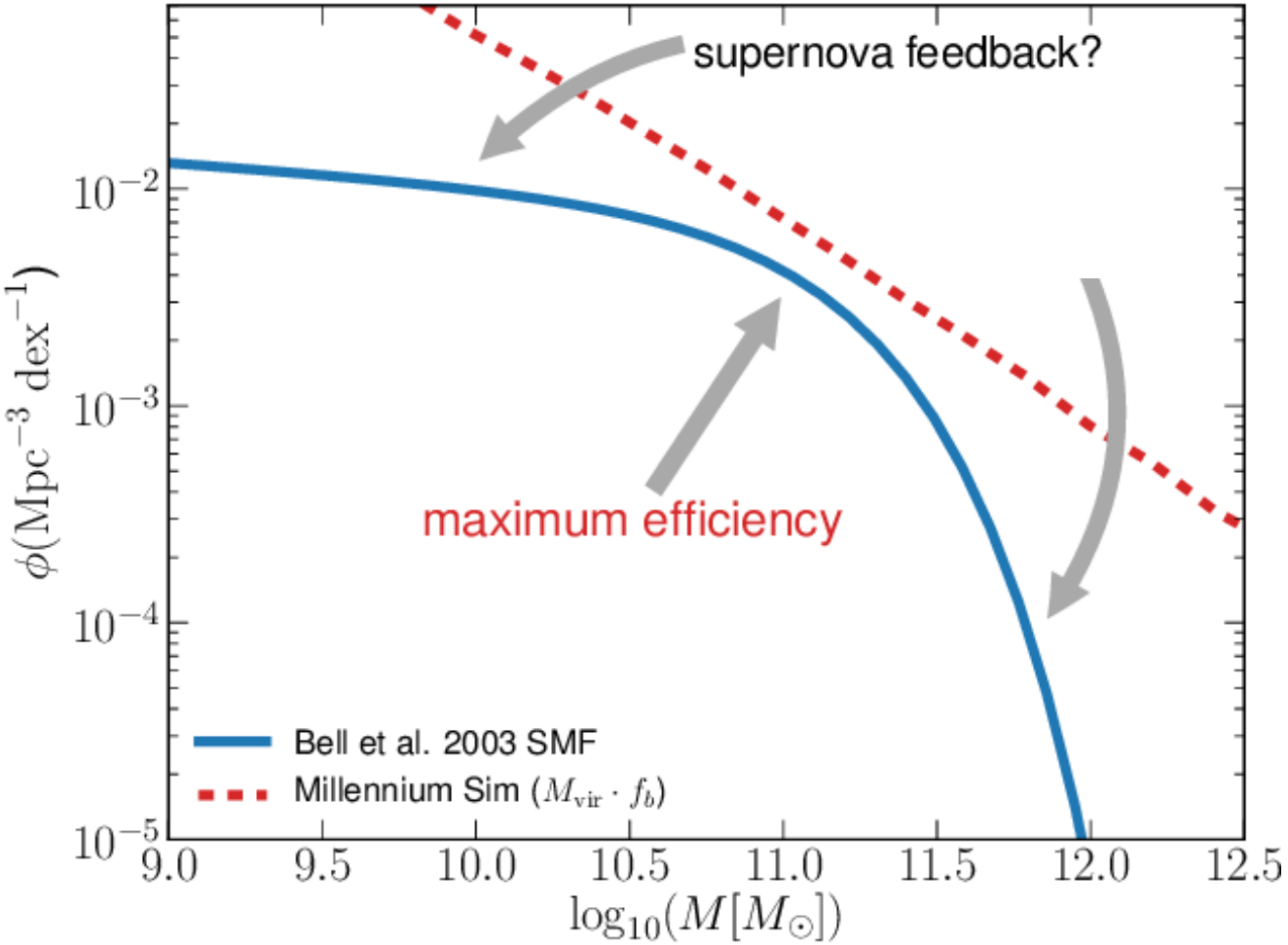
$\alpha \approx$ -1.94 @z=2.2-3 to $\alpha \approx$ -1.56 @z=1.-1.6
(Alavi et al 2016)

Origin of strong magnetic fields outside halos

- Damped Lyman-alpha systems (DLAs) at high z have 2-50 μG field (Wolfe 1992)
- Outside groups and clusters of galaxies there is 0.1-1 mG magnetic field (Bonafede+2013, Murgia+2004)
- magnetic field 0.3-0.5 μG in bridges linking clusters (Balboni+2023, O'Sullivan+2019)

Cen 2024, PNAS, 121 (35) e2402435121

But have supernovae already solved that problem?



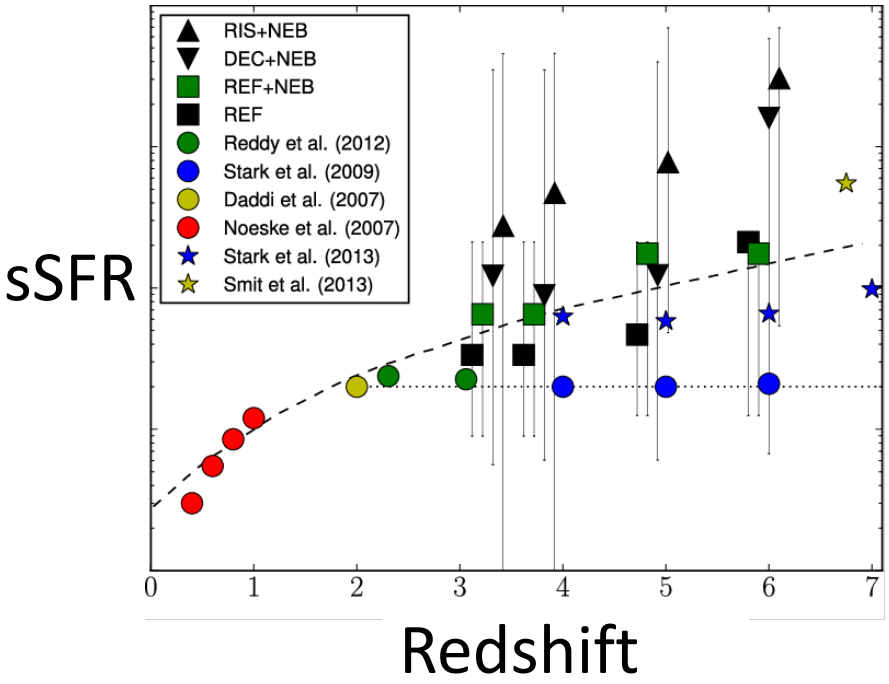
Is supernova feedback in the right direction even?

- when supernova feedback is supposed to be strongest at z>2,

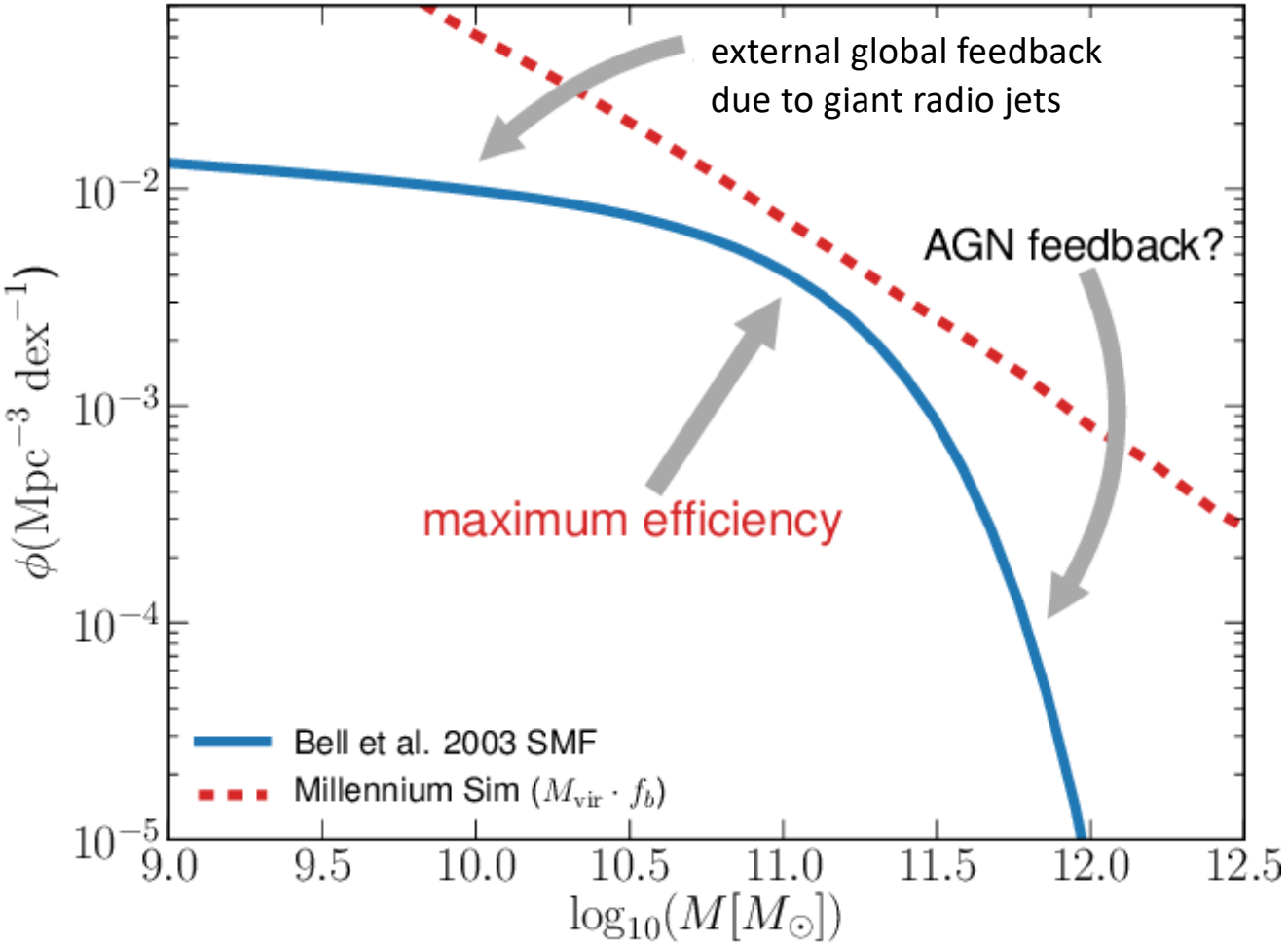
LF has a very steep (close to -2) slope,

- when supernova feedback is supposed to be strongest at z<2

LF has a very flat (close to -1) slope,



Ok, well, you still need the AGN feedback, right?



not really?

But I have believed so for so long

Let us put (religious) beliefs aside and

look at some of the observational evidence

Let us look at evidence of AGN feedback: central SF

Observations show significant central star formation enhancements galaxies with quasars,

not the way around

Where is negative AGN feedback?

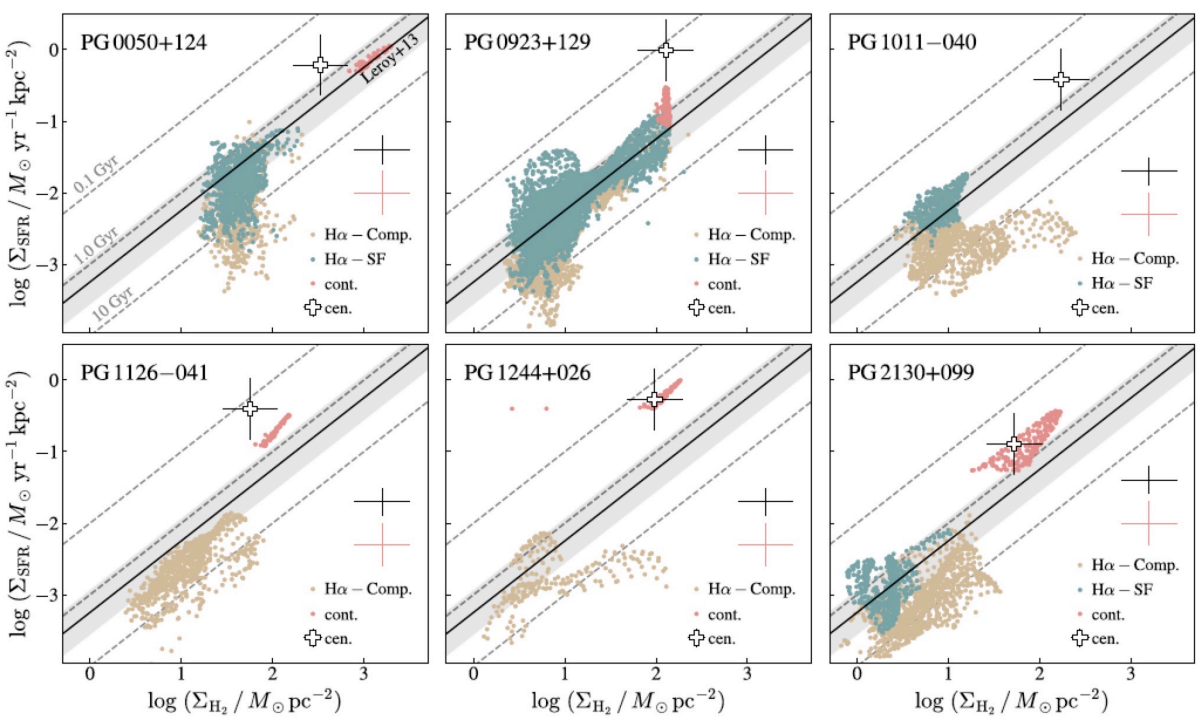


Figure 6. The PG quasar host galaxies in the Kennicutt–Schmidt diagram (Kennicutt 1998a). The red points show the Σ_{SFR} values estimated from the rest-frame 230 GHz continuum data. We show with green circles the MUSE pixels classified as star-forming, while the other pixels are represented by brown circles. The plus sign presents the average host galaxy central value computed over the host galaxy area where we miss the optical light emission owing to AGN deblending flux oversubtraction. The solid line shows the best-fit values of t_{dep} derived by Leroy et al. (2013) for local inactive galaxies, with the shaded region corresponding to the 1σ uncertainty. The dashed lines represent values of constant t_{dep}, as labeled in the top left panel. The regions with obscured and unobscured star formation activity are characterized by t_{dep} values similar to or slightly higher than those measured from the inactive systems, indicating starburst-like activity. The black and red colored error bars located above the legend correspond to the typical 1σ uncertainty of the Hα- and continuum-based pixel-wise data.

Evidence of AGN feedback: molecular gas

molecular gas amount
is independent of
quasar luminosity

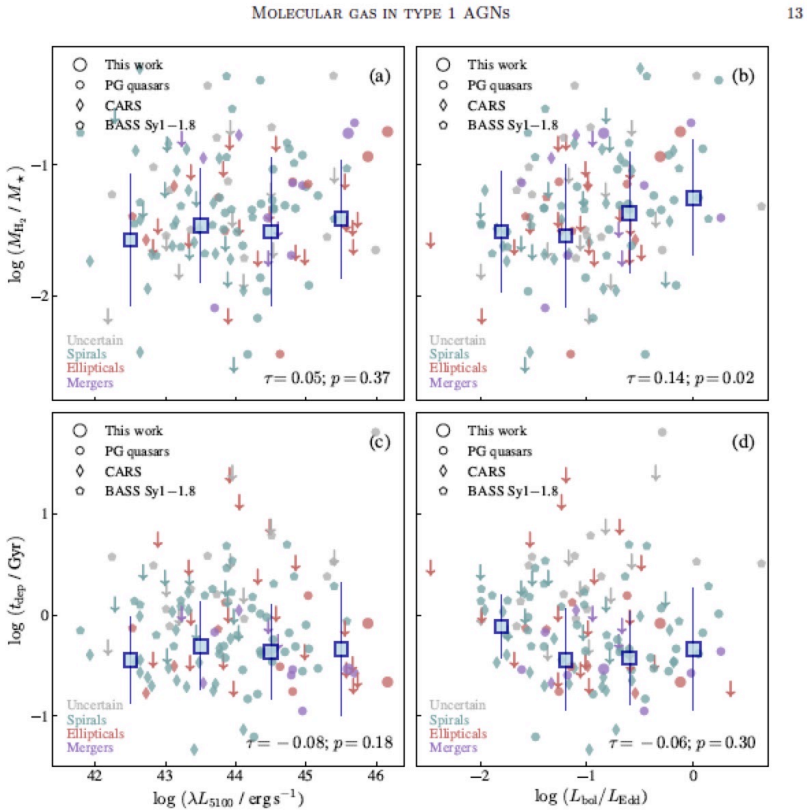


Figure 9. Host galaxy molecular gas properties as a function of AGN properties. The molecular gas fraction (M_{H_2}/M_*) dependence with (a) λL_{5100} and (b) Eddington ratio. Panels (c) and (d) show similar dependence on AGN properties, but for the molecular gas depletion time (M_{H_2}/SFR). In all panels, the data are colored by host galaxy morphology, and the blue squares correspond to median M_{H_2}/M_* or t_{dep} values computed in 0.6 dex λL_{5100} and 0.3 dex L_{bol}/L_{Edd} bins, respectively. The arrows correspond to 3σ upper limits.

Molina, Ho, et al 2023b

Evidence of AGN feedback: radio loudness dependence

star formation rate is independent of radio loudness

i.e., radio jets internal negative feedback is not widespread, either

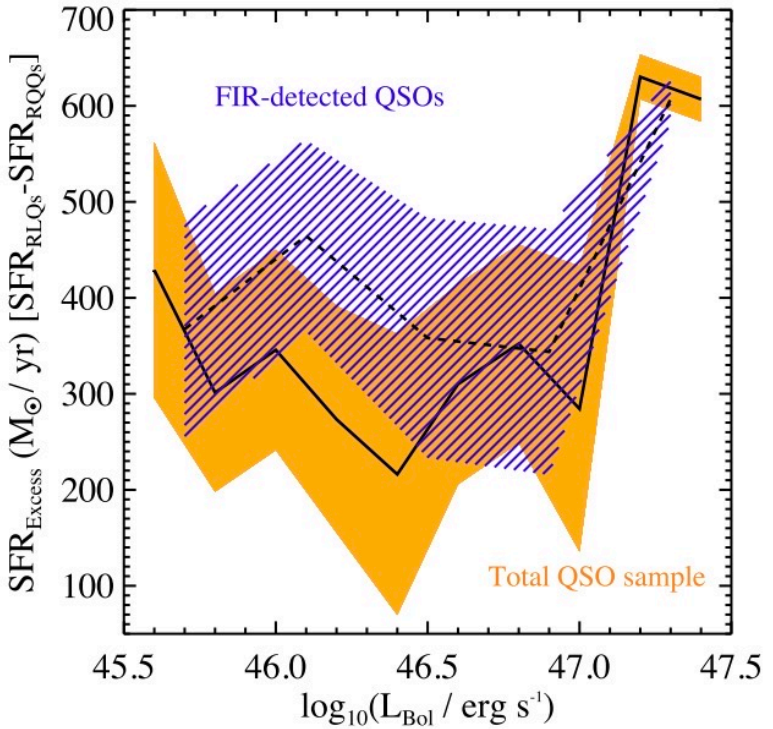


Figure 11. SFR excess between RLQs and RQQs as a function of bolometric luminosity for the total QSO sample (orange) and the FIR detected QSO sample (blue). The solid and dashed lines represent the weighted mean SFR excess and the coloured areas the 1σ error for the total QSO sample and the FIR-detected QSO sample, respectively.

Kalfountzou et al 2017

kinetic pressure of ISM: no evidence of negative AGN feedback

The kinetic pressure of ISM in galaxies with and without QSOs is similar.

Where is negative AGN feedback?

Fei et al 2024, arXiv:2409.15611

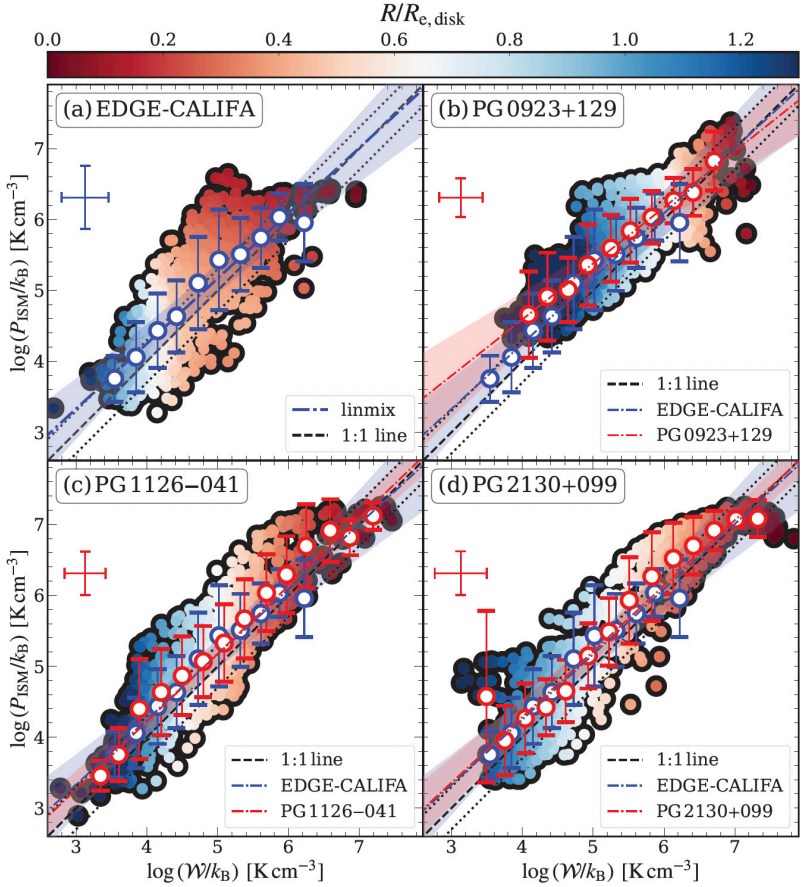


Figure 9. The relationship between the kinetic pressure of the ISM ($P_{\rm ISM}$) and the weight of the ISM ($\mathcal{W}$) for inactive galaxies (*panel (a)*) and for quasar host galaxies (*panel (b,c,d)*). Each data point represents a specific pixel. The blue circles illustrate the mean values of $P_{\rm ISM}$ for normal star-forming galaxies within 0.3 dex $\mathcal{W}$ bins, while red circles denote that for PG quasars. Error bars indicate the standard deviation of $P_{\rm ISM}$ within each $\mathcal{W}$ bin. The black dashed line represents the line of equality, with an associated scatter of 0.3 dex by the dotted line. The blue dash-dotted line represents the fitting result obtained through the usage of `linmix`, with uncertainties represented by the blue shaded region.

Is there enough AGN feedback energy overall?

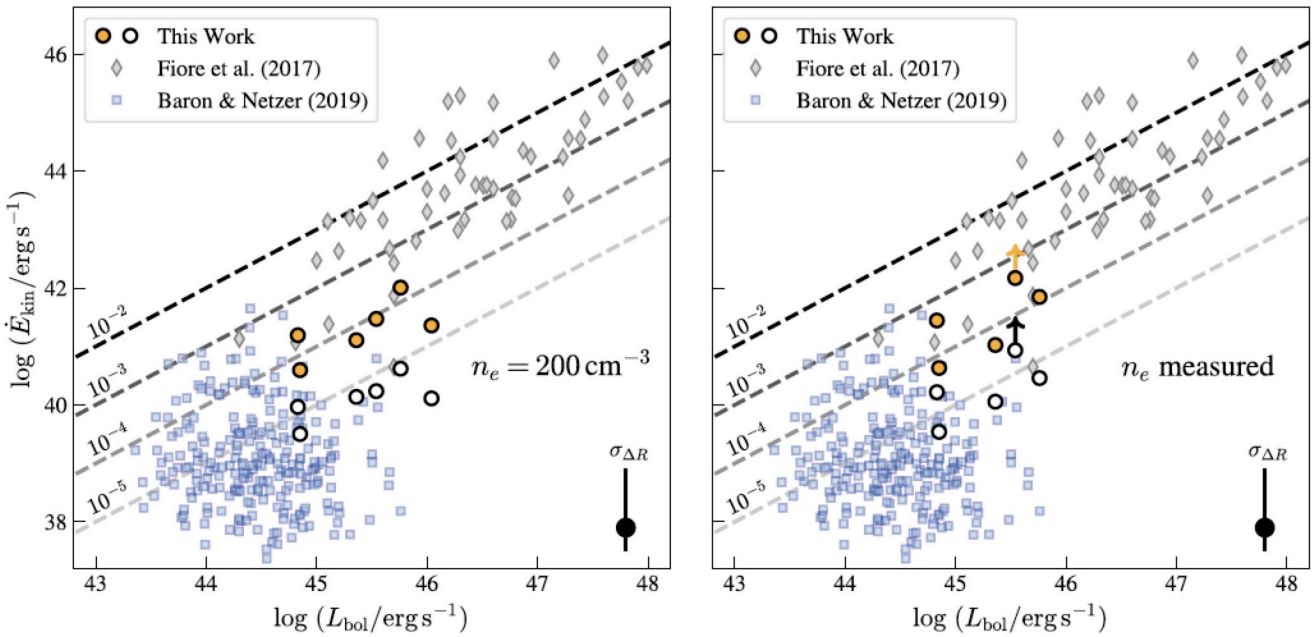


Figure 11. The outflow kinetic injection rate as a function of bolometric luminosity. The data are color-coded as in Figure 10. (Left) Kinetic injection rates compu by adopting $n_e = 200\ \mathrm{cm}^{-3}$. The vertical bar in the bottom right corner represents the systematic uncertainty associated with our assumed shell thickness. The dasl lines demarcate constant ratios of $\dot{E}_{\mathrm{kin}}/L_{\mathrm{bol}}$. (Right) Same as the left panel, but using values of n_e estimated from the observed [S II] doublet (Section 4.2.1). PG 2130+099, we only present upper limits assuming $n_e = 40\ \mathrm{cm}^{-3}$, as shown by upward-pointing arrows attached to the corresponding data points. We do not sh PG 1211+143, because it has an unconstrained value for the outflow n_e. Only PG 0050+124 presents an $\dot{E}_{\mathrm{kin}}/L_{\mathrm{bol}}$ value similar to the lower bound of those repor by Fiore et al. (2017).

4. Assuming that the local velocity dispersion enhancements reflect the interaction between the AGN-driven outflow and the host galaxy ISM, we compute ionized gas mass-outflow rates $\dot{M}_{\mathrm{out}} \approx 0.008$–$1.6\,M_{\odot}\ \mathrm{yr}^{-1}$ and kinetic injection powers $\dot{E}_{\mathrm{kin}}/L_{\mathrm{bol}} \lesssim 10^{-3}$. These values are substantially lower than those expected from the empirical correlations of Fiore et al. (2017), but they agree better with the estimates of Baron & Netzer (2019) and Rojas et al. (2020) for AGNs with similar and lower bolometric luminosities.

Present obs see $L_{kinetic}/L_{bol} < 10^{-3}$

significantly lower than from supernovae as a whole

This is much lower than 5×10^{-2} that was traditionally assumed.

Molina, Ho, et al 2022

Conclusions

- **External global feedback of giant radio lobes has the potential to help cure the ills of galaxy formation simulations.**
- **Systematic observational evidence of internal AGN negative feedback on star-forming galaxies is scarce.**
- **Postulated AGN feedback strength in simulation is not supported by evidence.**
- **Supernova feedback differentiates among varying mass galaxies apparently in the wrong direction.**

